


Spiral magnetic field and bound states of vortices in noncentrosymmetric superconductors

Albert Samoilenka  and Egor Babaev

Department of Physics, KTH-Royal Institute of Technology, SE-10691, Stockholm, Sweden

 (Received 31 March 2020; revised 25 July 2020; accepted 3 November 2020; published 25 November 2020)

We discuss the unconventional magnetic response and vortex states arising in noncentrosymmetric superconductors with chiral octahedral and tetrahedral (O or T) symmetry. We microscopically derive Ginzburg-Landau free energy. It is shown that due to spin-orbit and Zeeman coupling magnetic response of the system can change very significantly with temperature. For sufficiently strong coupling this leads to a crossover from type-I superconductivity at elevated temperature to vortex states at lower temperature. The external magnetic field decay in such superconductors does not have the simple exponential law. We show that in the London limit, magnetic field can be solved in terms of complex force-free fields \vec{W} , which are defined by $\nabla \times \vec{W} = \text{const} \vec{W}$. Using that we demonstrate that the magnetic field of a vortex decays in spirals. Because of such behavior of the magnetic field, the intervortex and vortex-boundary interaction becomes nonmonotonic with multiple minima. This implies that vortices form bound states with other vortices, antivortices, and boundaries.

DOI: [10.1103/PhysRevB.102.184517](https://doi.org/10.1103/PhysRevB.102.184517)

I. INTRODUCTION

Macroscopic magnetic and transport properties of superconductors have a significant degree of universality. For ordinary superconductors, the magnetic field behavior in the simplest case is described by the London equation [1–3]

$$\nabla^2 \vec{B} = \frac{1}{\lambda^2} \vec{B}. \quad (1)$$

This dictates that an externally applied magnetic field \vec{B} decays exponentially in the superconductor at the characteristic length scale called magnetic field penetration length λ . The equation relating the supercurrent to magnetic field $\nabla \times \vec{B} = \vec{J}$ dictates that the supercurrent should decay with the same exponent. Within the standard picture, this type of behavior describes the magnetic field near superconducting boundaries and in vortices, with microscopic detail, only affecting the coefficient λ . The single length scale associated with magnetic field behavior enables the Ginzburg-Landau classification of superconductors [4] by a single parameter: the ratio of λ to the coherence length (the characteristic length scale of density variation ξ). Within this classification, there are two types of superconductors, the type II that exists for $\lambda/\xi > 1$ allows stable vortices that interact repulsively, and in the type I, $\lambda/\xi < 1$ the vortices interact attractively and are not stable.

However, a simple two-length-scales-based classification of superconducting states cannot be complete. One counterexample is multicomponent materials, where there are several coherence lengths [5–9]. Moreover, there can be several magnetic field penetration lengths [10]. This multiscale physics gives nontrivial intervortex interaction and results in distinct magnetic properties.

How universal is the magnetic response in single-component systems? Here, we focus on magnetic and vortex properties of single-component systems in a crystal that lacks inversion symmetry. There are many discovered materials where superconductivity occurs in such crystals [11–16]. Then, (1) does not necessarily apply since symmetry now allows for noncentrosymmetric terms.

Indeed, Ginzburg-Landau (GL) free-energy functionals describing these, so-called noncentrosymmetric, superconducting systems were demonstrated to feature various new terms [11]. These include contributions that are linear in the gradients of the superconducting order parameter and the magnetic field \vec{B} . It principally revises the simplest London model (1) where such terms are forbidden on symmetry grounds. Depending on the symmetry of the material, the free energy can feature scalar and vector products of these fields of the form $\propto K_{ij} B_i J_j$, where $i = x, y, z$, $\vec{J} \propto \text{Re}[\psi^* D\psi]$, D is the covariant derivative and ψ is the order parameter, and K_{ij} are coefficients, which form depends on crystal symmetry [11]. Correspondingly, while in ordinary superconductors the externally applied field decays monotonically, in a Meissner state in a noncentrosymmetric superconductor it can have a spiral decay [11, 17–21]. This raises the question of the nature of topological excitations in such materials [11, 18–23]. The main goal of this paper is to investigate vortex solutions, their interaction, and the magnetic response of a superconductor where there is no inversion symmetry in an underlying crystal lattice.

Published by the American Physical Society under the terms of the [Creative Commons Attribution 4.0 International license](https://creativecommons.org/licenses/by/4.0/). Further distribution of this work must maintain attribution to the author(s) and the published article's title, journal citation, and DOI. Funded by [Bibsam](https://www.bibsam.org/).

Structure of the paper

In Sec. II we discuss the microscopic derivation of the Ginzburg-Landau (GL) model. A reader who is not interested in technical details can proceed directly to Sec. III. In Sec. III, by rescaling we cast the GL model in a representation that is more convenient for calculations and analysis. In Sec. IV we describe a method that solves the hydromagnetostatics of a noncentrosymmetric superconductor in the London limit in terms of complex force-free fields. A reader not interested in the analytical detail can proceed directly to the next section. In Sec. V we obtain analytic and numerical vortex configurations with a spiral magnetic field. In Sec. VI we calculate the temperature dependence of the single vortex energy to show how a crossover to type-1 superconductivity appears at elevated temperatures in a class of noncentrosymmetric superconductors. In Sec. VII we consider intervortex forces and show that system forms vortex-vortex and vortex-antivortex bound states. In Sec. VIII we consider the problem of a vortex near a boundary of noncentrosymmetric superconductor and show that vortex forms bound states with it.

II. MICROSCOPIC DERIVATION OF THE GINZBURG-LANDAU MODEL

Here, we present a microscopic derivation of the GL model in the case of chiral octahedral O or equivalently tetrahedral T symmetry from the microscopic model. A reader, not interested in the technical derivation of the model, can skip this section and directly proceed to the next sections that analyze the physical properties of the model.

A. Unbounded free energy in the minimal extension of the GL model

Typically, quoted phenomenological GL models have unphysical unboundedness of the energy from below [24]. For example, the model presented in Chap. 5 of [11] is given by energy density equal to usual GL model plus $K_{ij}B_iJ_j$ term. To see that energy is unbounded, it is sufficient to consider constant and real order parameter ψ . Then, energy density is given by $\frac{\bar{B}^2}{2} + \psi^2\bar{A}^2 - \psi^2K_{ij}B_iA_j + V(\psi)$, where V is potential. Consider the case of O or T symmetry given by $K_{ij} = \delta_{ij}K$. Then, inserting Chandrasekhar-Kendall function [25] as $\vec{B} = K\psi^2\vec{A}$ we obtain the energy density

$$F = \left[1 - \frac{K^2\psi^2}{2} \right] \psi^2\bar{A}^2 + V(\psi) \quad (2)$$

which is unbounded from below. That can be seen as follows: by increasing $\psi > \frac{\sqrt{2}}{K}$ and setting $\bar{A}^2 \rightarrow \infty$ one obtains infinitely negative energy density. Similarly, consider, for example, the case of C_{4v} symmetry, which corresponds to Rashba spin-orbit coupling $K_{ij}B_iJ_j = K(\vec{B} \times \vec{J})_z$. Then, we can set $\vec{A} = e^{-K\psi^2z}(\text{const}_x, \text{const}_y, 0)$. This leads to the same unbounded energy density equation (2).

The unboundedness of the model is associated with divergence of $|\psi|$ and $|\vec{B}|$. However, some of the previous works that derived the GL model assuming a finite uniform magnetic field \vec{B} [11,20,26] obtained the term $|\psi|^2\vec{B}^2$. This term in principle can make GL free energy bounded from below if

the assumption of constant $|\vec{B}|$ is lifted. Motivated by this problem, we proceed to derive the GL model with nonuniform \vec{B} aiming to obtain a microscopically justified effective model with a bounded energy.

B. Microscopic model

We will focus on the simplest case with the BCS-type local attractive interaction given by strength $V > 0$ but will include a general space-dependent magnetic field \vec{B} . Interaction is regularized by Debye frequency ω_D such that only electrons with Matsubara frequency $< \omega_D$ are interacting. We start from the continuous-space fermionic model in path-integral formulation, given by the action S and partition function Z :

$$S = \int_0^{\frac{1}{T}} d\tau \int_{-\infty}^{+\infty} d\vec{x} \sum_{\alpha, \beta = \uparrow, \downarrow} a_{\alpha}^{\dagger}(\mathbf{h} \cdot \boldsymbol{\sigma}_{\alpha\beta})a_{\beta} - Va_{\uparrow}^{\dagger}a_{\downarrow}^{\dagger}a_{\downarrow}a_{\uparrow},$$

$$Z = \int D[a^{\dagger}, a]e^{-S}, \quad (3)$$

where T is temperature and $a_{\alpha}(\tau, \vec{x})$, $a_{\alpha}^{\dagger}(\tau, \vec{x})$ are Grassman fields, which depend on imaginary time τ , three-dimensional space coordinates \vec{x} , and spin α . They correspond to fermionic creation and annihilation operators and

$$\mathbf{h} \equiv (\partial_{\tau} + E - \mu, \vec{h}), \quad \boldsymbol{\sigma}_{\alpha\beta} \equiv (\delta_{\alpha\beta}, \vec{\sigma}_{\alpha\beta}),$$

$$\vec{h} \equiv \vec{\gamma} - \mu_B\vec{B}(\vec{x}), \quad (4)$$

where $\vec{\sigma}_{\alpha\beta} \equiv ((\sigma_1)_{\alpha\beta}, (\sigma_2)_{\alpha\beta}, (\sigma_3)_{\alpha\beta})$ are Pauli matrices, e is electron charge, μ is chemical potential, and μ_B is Bohr magneton. Single-electron energy is $E[-i\nabla - e\vec{A}(\vec{x})]$ with $E(0) = 0$, which is $E(k) = \frac{k^2}{2m}$ for quasifree electrons. However, in our derivation, we keep $E(k)$ in general form, also suitable for band electrons. The only term responsible for noncentrosymmetric nature of the system is spin-orbit coupling $\vec{\gamma}(-i\nabla - e\vec{A}(\vec{x}))$.

Let us now consider the case of cubic O or T symmetry with simplest coupling $\vec{\gamma}(\vec{a}) = \gamma_0\vec{a}$. We will focus on the standard situation where the macroscopic length scale λ , over which the quantities \vec{A} , \vec{B} change, is much larger than Fermi length scale $\propto 1/k_F$, where k_F is Fermi momenta. We assume that the following inequalities hold:

$$\mu \gg \omega_D \gg T_c, \quad \gamma_0k_F \gg \omega_D \gg \mu_B B, \quad (5)$$

where T_c is the critical temperature of a superconductor to a normal phase transition. We perform Hubbard-Stratonovich transformation by introducing auxiliary bosonic field $\Delta(\tau, \vec{x})$. Hence, up to a constant, the interaction term becomes

$$e^{V \int d\tau d\vec{x} a_{\uparrow}^{\dagger} a_{\downarrow}^{\dagger} a_{\downarrow} a_{\uparrow}} = \int D[\Delta^{\dagger}, \Delta] e^{-\int d\tau d\vec{x} (\frac{\Delta^{\dagger}\Delta}{V} + \Delta^{\dagger} a_{\uparrow} a_{\downarrow} + \Delta a_{\downarrow}^{\dagger} a_{\uparrow}^{\dagger})}. \quad (6)$$

Next, by introducing $b \equiv (a_{\uparrow}, a_{\downarrow}, a_{\uparrow}^{\dagger}, a_{\downarrow}^{\dagger})^T$ the partition function (3) can be written as

$$Z = \int D[\Delta^{\dagger}, \Delta] D[b] e^{-\int d\tau d\vec{x} (\frac{1}{2} b^T H b + \frac{\Delta^{\dagger}\Delta}{V})}, \quad (7)$$

where we have the matrix $H = H_0 + \Lambda$ with

$$H_0 = \begin{pmatrix} 0 & -\hat{\mathbf{h}}^T \\ \hat{\mathbf{h}} & 0 \end{pmatrix}, \quad \Lambda = \begin{pmatrix} \hat{\delta}^\dagger & 0 \\ 0 & \hat{\delta} \end{pmatrix}. \quad (8)$$

The symbol with a hat denotes 2×2 matrices defined by $\hat{\mathbf{h}} = \boldsymbol{\sigma} \cdot \mathbf{h}$ and $\hat{\delta} = \boldsymbol{\sigma} \cdot (0, 0, i\Delta, 0)$. Note that for any function of operators f , transposition is defined as $f^T(\partial_\tau, \nabla) = f(-\partial_\tau, -\nabla)$. Integrating out fermionic degrees of freedom b , by performing Berezin integration in (7), we obtain

$$Z = \int D[\Delta^\dagger, \Delta] e^{\frac{1}{2} \ln \det H - \int d\tau d\vec{x} \frac{\Delta^\dagger \Delta}{V}}. \quad (9)$$

In the mean-field approximation, one assumes that Δ does not depend on τ (i.e., it is classical) and does not fluctuate thermally. Hence, free energy is given by

$$F = TS = \int d\vec{x} \frac{|\Delta|^2}{V} - \frac{T}{2} \text{Tr} \ln H. \quad (10)$$

By Tr here and below we mean matrix trace tr and integration $\int d\vec{x} d\tau$. To obtain the GL model we need to expand the second term in (10) in powers and derivatives of the field Δ :

$$\text{Tr} \ln H = \text{Tr} \ln (1 + H_0^{-1} \Lambda) = \sum_{\nu=1}^{\infty} \frac{(-1)^{\nu+1}}{\nu} \text{Tr} [(\hat{\mathbf{g}} \hat{\delta} \hat{\mathbf{g}}^T \hat{\delta}^\dagger)^\nu], \quad (11)$$

where the first equality is defined, up to constant in Δ and $\hat{\mathbf{g}}$, through

$$H_0^{-1}(\tau, \tau', \vec{x}, \vec{x}') = \begin{pmatrix} 0 & \hat{\mathbf{g}} \\ -\hat{\mathbf{g}}^T & 0 \end{pmatrix} \Rightarrow \hat{\mathbf{h}} \hat{\mathbf{g}} = \delta(\vec{x} - \vec{x}') \delta(\tau - \tau'). \quad (12)$$

Note that in Eq. (11) matrices are multiplied and integrated inside the trace, for example, $\hat{\mathbf{g}} \hat{\delta} \hat{\mathbf{g}}^T \hat{\delta}^\dagger \equiv \int d\vec{x}' d\tau' \hat{\mathbf{g}}(\tau, \tau', \vec{x}, \vec{x}') \hat{\delta}(\vec{x}') \hat{\mathbf{g}}^T(\tau', \tau'', \vec{x}', \vec{x}'') \hat{\delta}^\dagger(\vec{x}'')$. Next, we define

$$\hat{\mathbf{g}} = e^{\phi(\vec{x}, \vec{x}') \hat{\mathbf{f}}} \quad (13)$$

so that for slowly changing \vec{A} , \vec{B} we get $\hat{\mathbf{h}}(-i\nabla - e\vec{A}(\vec{x})) \hat{\mathbf{g}} \simeq e^{\phi} \hat{\mathbf{h}}(-i\nabla) \hat{\mathbf{f}}$ with $\phi(\vec{x}, \vec{x}') \simeq ie\vec{A}(\vec{x})(\vec{x} - \vec{x}')$. The Fourier transform for \mathbf{g} , $\hat{\mathbf{g}} = \boldsymbol{\sigma} \cdot \mathbf{g}$, is given by

$$\begin{aligned} \mathbf{g}(\tau - \tau', \vec{x} - \vec{x}') &= e^{ie\vec{A}(\vec{x})(\vec{x} - \vec{x}')} T \sum_{w_n}^{|w_n| < \omega_D} \frac{1}{(2\pi)^3} \\ &\times \int d\vec{k} e^{-iw_n(\tau - \tau')} e^{i\vec{k} \cdot (\vec{x} - \vec{x}')} \mathbf{f}(w_n, \vec{k}), \end{aligned} \quad (14)$$

where $w_n = 2\pi T(n + \frac{1}{2})$ is Matsubara frequency. Here, we used the fact that only electrons with frequency w_n smaller than Debye frequency ω_D are interacting, and that $\hat{\mathbf{f}}$ is a solution of the equation $\hat{\mathbf{h}} \hat{\mathbf{f}} = 1$. By using the Fourier transformed $\mathbf{h}(w_n, \vec{k}) = [-iw_n + E(k) - \mu, \gamma_0 \vec{k} - \mu_B \vec{B}]$ we obtain

$$\mathbf{f} = \frac{\mathbf{h}}{\mathbf{h} \cdot \mathbf{h}}, \quad (15)$$

where $\underline{\mathbf{h}} \equiv (h_0, -\vec{h})$ if $\mathbf{h} = (h_0, \vec{h})$. We can rewrite \mathbf{f} as

$$\begin{aligned} \mathbf{f} &= \frac{1}{2}(\underline{\mathbf{f}}_+ + \underline{\mathbf{f}}_-), \quad \underline{\mathbf{f}}_\pm = G_\pm \mathbf{s}, \\ G_\pm &= \frac{1}{h_0 \pm h}, \quad \mathbf{s} = (1, \vec{e}_h), \end{aligned} \quad (16)$$

where we use the notations $h \equiv |\vec{h}|$ and $\vec{e}_h \equiv \frac{\vec{h}}{h}$.

C. Minimal set of terms in the GL expansion for the noncentrosymmetric materials

1. Second-order terms

First, we examine the terms occurring in the second order. To that end, by using the (14) and substituting $\Delta^*(\vec{x}') = e^{(\vec{x}' - \vec{x}) \cdot \nabla} \Delta^*(\vec{x})$ we compute $\nu = 1$ term in (11) which is second order in Δ :

$$\begin{aligned} \text{Tr}[\hat{\mathbf{g}} \hat{\delta} \hat{\mathbf{g}}^T \hat{\delta}^\dagger] &= 2 \text{Tr}[(\mathbf{g} \Delta) \cdot (\underline{\mathbf{g}}^T \Delta^*)] \\ &= 2 \int d\vec{x} d\tau d\vec{x}' d\tau' \Delta(\vec{x}) \mathbf{g}(\tau', \tau, \vec{x}', \vec{x}) \\ &\quad \cdot \underline{\mathbf{g}}^T(\tau, \tau', \vec{x}, \vec{x}') \Delta^*(\vec{x}') \\ &= 2 \int d\vec{x} \Delta(\vec{x}) \sum_{w_n} \int \frac{d\vec{k}}{(2\pi)^3} \mathbf{f}(w_n, \vec{k}) \\ &\quad \cdot \underline{\mathbf{f}}(-w_n, -\vec{k} + D) \Delta^*(\vec{x}), \end{aligned} \quad (17)$$

where the operator $D = -i\nabla - 2e\vec{A}(\vec{x})$ is acting only on the gap field $\Delta^*(\vec{x})$. The goal here is to simplify $\mathbf{f} \cdot \underline{\mathbf{f}}$ term in (17), where the prime means dependence on $(-w_n, -\vec{k} + D)$. Hence, using that $\gamma_0 k_F \gg \mu_B B$ we approximate

$$|\vec{h}| \simeq \gamma_0 k - \vec{e}_k \cdot \mu_B \vec{B}, \quad |\vec{h}'| \simeq \gamma_0 k + \vec{e}_k \cdot (\mu_B \vec{B} - \gamma_0 D). \quad (18)$$

Then it is easy to show that up to the second order in $\frac{D}{k_F}$ and $\frac{\mu_B B}{\gamma_0 k_F}$, $\mathbf{s} \cdot \mathbf{s}' \simeq 0$ and $\mathbf{s} \cdot \underline{\mathbf{s}}' \simeq 2$. Hence, using (16) we obtain

$$\mathbf{f} \cdot \underline{\mathbf{f}} \simeq \frac{1}{2}(G_- G'_- + G_+ G'_+). \quad (19)$$

When summing over w_n , contribution to integration over momenta in (17) mainly comes from a thin shell near Fermi momenta k_{aF} because the interaction is cut off by Debye frequency. This shell has the width $\simeq \omega_D$:

$$\varepsilon_a(k_{aF}) = 0, \quad \text{with } \varepsilon_a \equiv E(k) + a\gamma_0 k - \mu, \quad (20)$$

where $a = \pm 1$ is the band index. Hence, we can approximate $E(-\vec{k} + D) \simeq E(k) - E'(k_{aF}) \vec{e}_k \cdot D$. By using $\mu \gg \omega_D$ and $\gamma_0 k_{aF} \gg \omega_D$, the integral in (17) can be estimated as

$$\begin{aligned} \int \frac{d\vec{k}}{(2\pi)^3} &\simeq N_a \int_{-\infty}^{+\infty} d\varepsilon_a \int \frac{d\Omega_k}{4\pi}, \quad N_a \equiv \frac{1}{2\pi^2} \frac{k_{aF}^2}{v_{aF}}, \\ v_{aF} &\equiv E'(k_{aF}) + a\gamma_0, \end{aligned} \quad (21)$$

where N_a is density of states at Fermi level, v_{aF} is Fermi velocity, and $d\Omega_k$ is solid angle. Then, we perform integration and Matsubara sum in (17) by using Eqs. (19), (21), and

$\omega_D \gg T$:

$$\sum_{w_n} \int \frac{d\vec{k}}{(2\pi)^3} \underline{f} \cdot \underline{f}' \simeq \sum_{a=\pm 1} \frac{N_a}{2T} \int \frac{d\Omega_k}{4\pi} \left[\ln \frac{\omega_D}{2\pi T} - \text{Re}'\Psi \left(\frac{1}{2} + i\vec{e}_k \cdot \frac{v_{aF}D - 2a\mu_B\vec{B}}{4\pi T} \right) \right], \quad (22)$$

where $\text{Re}'X \equiv \frac{1}{2}(X + X^\dagger)$ and Ψ is digamma function. Next, we expand in D , \vec{B} and average over \vec{e}_k in Eq. (22). Combining the result with Eqs. (17), (11), and (10) and integrating by parts with $\nabla\vec{A} = 0$, we obtain the part of the free energy which is second order in Δ :

$$F_2 = \int d\vec{x} \left[\alpha |\Delta|^2 + \sum_{a=\pm 1} K_a |(v_{aF}D^* - 2a\mu_B\vec{B})\Delta|^2 \right],$$

$$\alpha = N \ln \frac{T}{T_c}, \quad T_c = \frac{2e^{\gamma_{\text{Euler}}}}{\pi} \omega_D e^{-\frac{1}{N\nu}},$$

$$K_a = \frac{7\zeta(3)}{6(4\pi T)^2} N_a, \quad N = \frac{N_+ + N_-}{2}. \quad (23)$$

Note that the kinetic term is split into two terms corresponding to different bands with covariant derivatives that apart from \vec{A} have \vec{B} . If one opens brackets, the only noncentrosymmetric term is proportional to difference of squares of Fermi momenta of two bands:

$$\propto (k_{-F}^2 - k_{+F}^2) \vec{B} \cdot (\Delta D \Delta^* + \Delta^* D^* \Delta). \quad (24)$$

2. Fourth-order term

As usual, at the fourth order, it is sufficient to retain only term $\propto |\Delta|^4$. Hence, we neglect \vec{A} , \vec{B} and difference in Δ^* . To that end, we consider $\nu = 2$ term in Eq. (11). By using Eq. (14) it can be written as

$$-\frac{1}{2} \text{Tr}[(\hat{g}\hat{\delta}\hat{g}^T\hat{\delta}^\dagger)^2] \simeq -\frac{1}{2} \sum_{w_n} \int d\vec{x} \frac{d\vec{k}}{(2\pi)^2} \text{tr}[(\hat{f}\hat{\delta}\hat{f}^T\hat{\delta}^\dagger)^2]$$

$$\simeq -\frac{1}{2} \int d\vec{x} |\Delta|^4 \sum_a N_a \sum_{w_n} \times \int_{-\infty}^{+\infty} \frac{d\varepsilon_a}{(w_n^2 + \varepsilon_a^2)^2}. \quad (25)$$

Here, to go to the second equality we used (16). By using Eqs. (25) and (10) we obtain the part of the free energy which is quartic in order parameter:

$$F_4 = \int d\vec{x} \beta |\Delta|^4, \quad \text{with } \beta = \frac{7\zeta(3)}{(4\pi T)^2} N. \quad (26)$$

The principal difference between the GL model of centrosymmetric and noncentrosymmetric material here is in the form of the gradient term in Eq. (23). Note that the frequently used phenomenological noncentrosymmetric GL models include only the cross term $\vec{B} \cdot \vec{J}$, that makes these models unbounded from below. The derived microscopic model solves this issue because the gradient term in (23) is a full square, i.e., is positively defined.

III. RESCALING AND PARAMETRIC DEPENDENCE OF THE MICROSCOPIC GL MODEL

In this section, we rescale the GL model to a simpler form that is analyzed below. The minimal, microscopically derived GL model for noncentrosymmetric superconductor reads as a sum of second-order F_2 and fourth-order F_4 terms, given by (23) and (26):

$$F = \int d\vec{x} \left[\frac{(\vec{B} - \vec{H})^2}{2} + \alpha |\Delta|^2 + \beta |\Delta|^4 + \sum_{a=\pm 1} K_a |(v_{aF}D^* - 2a\mu_B\vec{B})\Delta|^2 \right]. \quad (27)$$

Importantly, the energy of the model, derived here, is bounded from below, i.e., the functional does not allow infinitely negative energy states. This is in contrast to the phenomenological model presented in Chap. 5 of [11], which has artificial unboundedness of the energy from below [24].

The microscopically derived model can be cast in a more compact form by introducing the new variables \vec{r} , ψ , F' , \vec{A}' and performing the following transformation:

$$\vec{x} = \frac{1}{\sqrt{-\alpha}} \left(\frac{\beta}{2e^2} \right)^{\frac{1}{4}} \vec{r}, \quad \Delta = \sqrt{\frac{-\alpha}{2\beta}} \psi, \quad F = \frac{\sqrt{-\alpha}}{2(2e^2)^{\frac{3}{4}} \beta^{\frac{1}{4}}} F',$$

$$\vec{A} = \frac{1}{2e} \frac{r}{x} \vec{A}'. \quad (28)$$

After dropping the prime, the rescaled GL free energy can be written as

$$F = \int d\vec{r} \left[\frac{(\vec{B} - \vec{H})^2}{2} + \sum_{a=\pm 1} \frac{|\mathcal{D}_a \psi|^2}{2\kappa_c} - |\psi|^2 + \frac{|\psi|^4}{2} \right],$$

$$\mathcal{D}_a \equiv i\nabla - \vec{A} - (\gamma + a\nu)\vec{B}, \quad (29)$$

where we define new parameters

$$\kappa_c = \sqrt{\frac{\beta}{2e^2}} \frac{1}{\sum_{a=\pm 1} K_a v_{aF}^2}, \quad \vec{H} = \frac{\sqrt{2\beta}}{-\alpha} \vec{H},$$

$$\gamma = \sqrt{-\alpha} \left(\sum_{a=\pm 1} a K_a v_{aF} \right) 2\mu_B \kappa_c \left(\frac{2e^2}{\beta} \right)^{\frac{3}{4}},$$

$$\nu = \sqrt{-\alpha} K_+ K_- \left(\sum_{a=\pm 1} v_{aF} \right) 2\mu_B \kappa_c \left(\frac{2e^2}{\beta} \right)^{\frac{3}{4}}. \quad (30)$$

Two conclusions can be drawn here:

(i) The noncentrosymmetric term (24) has the prefactor γ that modifies the gradient term. It means that the sign of γ determines whether left- or right-handed states are preferable. The term is proportional to microscopic spin-orbit coupling $\gamma \propto \gamma_0$ if $\gamma_0 k_F \ll \mu$. On the other hand, the parameter ν appears due to the coupling to the Zeeman magnetic field.

(ii) The parameters γ , ν are proportional to $\sqrt{-\alpha}$ and hence for $T \rightarrow T_c$ we get γ , $\nu \rightarrow 0$. Here, T_c is the critical temperature, defined in (23) so that $\alpha \propto \ln \frac{T}{T_c}$. Note that the characteristic parameter κ_c does not have the same meaning as the standard Ginzburg-Landau parameter. However, asymptotically, in the limit $T \rightarrow T_c$ the noncentrosymmetric

superconductor will behave as a usual superconductor with GL parameter κ_c .

Varying (29) with respect to ψ^* , ψ and \vec{A} we obtain the following Ginzburg-Landau (GL) equations:

$$\begin{aligned} \sum_a \frac{D_a^2 \psi}{2\kappa_c} - \psi + |\psi|^2 \psi &= 0, \\ \sum_a \frac{(D_a^2 \psi)^*}{2\kappa_c} - \psi^* + |\psi|^2 \psi^* &= 0, \\ \nabla \times \left[\vec{B} - \vec{H} - \sum_a (\gamma + av) \vec{J}_a \right] &= \sum_a \vec{J}_a \end{aligned} \quad (31)$$

with $\vec{J}_a = \frac{\text{Re}(\psi^* D_a \psi)}{\kappa_c}$ and boundary conditions for unitary vector \vec{n} orthogonal to the boundary:

$$\begin{aligned} \vec{n} \cdot \sum_a D_a \psi &= 0, \\ \vec{n} \cdot \sum_a (D_a \psi)^* &= 0, \quad \vec{n} \times \left[\vec{B} - \vec{H} - \sum_a (\gamma + av) \vec{J}_a \right] \\ &= 0. \end{aligned} \quad (32)$$

IV. AN ANALYTICAL APPROACH FOR SOLUTIONS IN THE LONDON LIMIT: MAGNETIC FIELD CONFIGURATION AS THE SOLUTION TO THE COMPLEX FORCE-FREE EQUATION

In this section, we develop an analytical method for treating Eq. (31). That will allow us to determine the magnetic field and current configurations in the London limit.

A. Decoupling of fields at linear level

First, we focus on asymptotic of Eq. (31) over uniform background $\psi = 1$. Namely, we set $\psi = (1 + \varepsilon)e^{i\phi}$ and assume that ε , \vec{B} , and $\vec{j} \equiv \nabla\phi + \vec{A} + \gamma\vec{B}$ are small. By linearizing the GL equations (31) in terms of them we obtain

$$\Delta\varepsilon - 2\kappa_c\varepsilon = 0, \quad \chi^2 \nabla \times \vec{B} + \gamma \nabla \times \vec{j} + \vec{j} = 0, \quad (33)$$

where $\chi = \sqrt{\frac{\kappa_c}{2} + \nu^2}$. This is accompanied by the boundary conditions (32):

$$\vec{n} \cdot \nabla\varepsilon = 0, \quad \vec{n} \cdot \vec{j} = 0, \quad \vec{n} \times \left[\chi^2 \vec{B} + \gamma \vec{j} - \frac{\kappa_c}{2} \vec{H} \right] = 0. \quad (34)$$

Note that the equation for the matter field ε has the same form as for usual superconductors. That allows us to define the coherence length as $\xi = \frac{1}{\sqrt{2\kappa_c}}$ so that it parametrizes the exponential law $\psi \propto e^{-x/\xi}$ how the matter field recovers from a local perturbation. Importantly, the equation for \vec{B} and \vec{j} is decoupled from the equation for ε at the level of linearized theory. That means that the London limit is a fully controllable approximation for a noncentrosymmetric superconductor with short coherence length. Namely, when the length scale of density variation ξ is much smaller than the characteristic length scale of the magnetic field decay and we are sufficiently far away from the upper critical magnetic field, so that vortex

cores do not overlap, the London model is a good approximation.

B. Analytical approach for solutions in the London limit in the presence of vortices

In the London approximation the order parameter is set to $\psi = 0$ at $r < \xi$ to model a core of a vortex positioned at $r = 0$. Away from the core it recovers to bulk value $\psi = e^{i\phi}$.

Taking the curl of the second equation in (33) we obtain an equation that determines configuration of the magnetic field:

$$\begin{aligned} [\chi^2 + \gamma^2] \nabla \times (\nabla \times \vec{B}) + 2\gamma \nabla \times \vec{B} + \vec{B} \\ = -\nabla \times \nabla\phi - \gamma \nabla \times (\nabla \times \nabla\phi). \end{aligned} \quad (35)$$

Far away from the vortex core, the right-hand side of (35) should be zero. By introducing a differential operator

$$\mathcal{L} = -\eta + \nabla \times \quad \text{with} \quad \eta \equiv \eta_1 + i\eta_2 = \frac{-\gamma + i\chi}{\gamma^2 + \chi^2}. \quad (36)$$

Equation (35) with zero on the right-hand side can be written as

$$\mathcal{L}\mathcal{L}^*\vec{B} = 0. \quad (37)$$

To simplify this equation, we introduce complex force-free field \vec{W} defined by $\nabla \times \vec{W} = \eta\vec{W}$ or, equivalently, by $\mathcal{L}\vec{W} = 0$. Using this and Eq. (37) we obtain that

$$\mathcal{L}^*\vec{B} = c\vec{W}, \quad (38)$$

where c is an arbitrary complex-valued constant. Subtracting the complex conjugate from (38) we obtain the solution for the magnetic field \vec{B} in terms of complex force-free field \vec{W} :

$$\vec{B} = \text{Re}\vec{W}. \quad (39)$$

Note that we absorbed multiplicative complex constant into the definition of \vec{W} in the last step.

To obtain a solution for \vec{W} , one can solve the equation $\mathcal{L}\vec{W} = 0$. However, it is more elegant to employ the trick used by Chandrasekhar and Kendall [25]. Namely, the solution for \vec{W} is made of auxiliary functions:

$$\vec{W} = \vec{T} + \frac{1}{\eta} \nabla \times \vec{T}, \quad \vec{T} = \nabla \times (\vec{v}f(\vec{r})), \quad \nabla^2 f + \eta^2 f = 0. \quad (40)$$

There is freedom in choosing \vec{v} : it can be set to, for example, $\vec{v} = \text{const}$ or $\vec{v} \propto \vec{r}$. We note that to make resulting equations simpler, if possible, it is convenient to satisfy $\vec{v} = \text{const} \in \text{Re}$, $|\vec{v}| = 1$, and $\vec{v} \cdot \nabla f = 0$. In this work we fix it to $\vec{v} = \vec{e}_z$ and hence set \vec{W} to

$$\vec{W} = \eta f \vec{e}_z - \vec{e}_z \times \nabla f. \quad (41)$$

In a London model a solution for a vortex is obtained by including a source term. Now, if we take into account the right-hand side of (35) the second equation in (40) should be modified to include source term δ , which we define by $\nabla^2 f + \eta^2 f = \eta\delta$. For multiple vortices with windings n_i , placed at different positions \vec{r}_i , we have

$$\nabla \times \nabla\phi = 2\pi \vec{e}_z \sum_i n_i \delta(x - x_i, y - y_i). \quad (42)$$

Equation (35) with nonzero right-hand side can be written as

$$\text{Re}[\mathcal{L}^*(\mathcal{L}\bar{W} - \eta\nabla \times \nabla\phi)] = 0. \quad (43)$$

From Eq. (41) we obtain that $\mathcal{L}\bar{W} = -\bar{e}_z\eta\delta$. Inserting it in Eq. (43) results in

$$\delta = -2\pi \sum_i n_i \delta(x - x_i, y - y_i). \quad (44)$$

This section can be summarized as follows: We justified taking the London limit by decoupling linearized matter field equation from magnetic field equation. We demonstrated that Eq. (35), that determines magnetic field of superconductor in the London limit, can be simplified to

$$\begin{aligned} \vec{B} &= \text{Re}\bar{W}, \quad \bar{W} = \eta f \bar{e}_z - \bar{e}_z \times \nabla f, \\ \nabla^2 f + \eta^2 f &= -2\pi \eta \sum_i n_i \delta(x - x_i, y - y_i). \end{aligned} \quad (45)$$

Note that this representation of \vec{B} in terms of complex force-free fields is *general*: i.e., it holds also for the usual centrosymmetric superconductor. But, as will be clear from the discussion below, it is particularly useful for noncentrosymmetric materials.

C. Calculation of the free energy of nontrivial configurations

An example where the London model yields important physical information is vortex energy calculations. That allows determining, for instance, lower critical magnetic fields and magnetization curves. Free-energy equation (29), up to a constant, can be written as

$$F = \int d\vec{r} \left[\frac{\chi^2}{\kappa_c} B^2 - \vec{B} \cdot \vec{H} + \frac{j^2}{\kappa_c} \right], \quad (46)$$

where \vec{j} is found from the second equation in (33) and curl of its definition $\nabla \times \vec{j} = \nabla \times \nabla\phi + \vec{B} + \gamma \nabla \times \vec{B}$. The formalism presented in this section allows a simple solution:

$$\vec{j} = \chi \text{Im}\bar{W}. \quad (47)$$

Hence, energy of *any* configuration can be written as

$$F = \int d\vec{r} \left[\frac{\chi^2}{\kappa_c} |\bar{W}|^2 - \text{Re}\bar{W} \cdot \vec{H} \right]. \quad (48)$$

Furthermore, by using Eq. (41), the energy (48) can be further simplified to

$$F = \int d\vec{r} \left[\frac{\chi^2}{\kappa_c} (|\nabla f|^2 + |\eta f|^2) - \text{Re}\bar{W} \cdot \vec{H} \right]. \quad (49)$$

We will use the formalism of this section below to analyze the physical properties of noncentrosymmetric systems.

V. STRUCTURE OF A SINGLE VORTEX

A. Analytical treatment in the London limit

Earlier, vortex solutions were obtained only as a series expansion [11,18], which did not exhibit any spiral structure of the magnetic field. In this section, we show how the method that we developed in (45) allows us to obtain an exact solution that turns out to be structurally different.

Consider a single vortex translationally invariant along the z direction and positioned at $x, y = 0$. Then, in order to obtain magnetic field we need to solve the second equation in (45):

$$\nabla^2 f + \eta^2 f = -2\pi \eta n \delta(x, y). \quad (50)$$

First, let us solve it with zero right-hand side. Then, (50) is just Helmholtz equation with complex parameter η . In polar coordinates ρ and θ its solution is $f = \sum_{j=-\infty}^{+\infty} c_j e^{ij\theta} H_j^{(1)}(\eta\rho)$, where we chose $H_j^{(1)}$, Hankel function of the first kind to obtain appropriate asymptotic $f \rightarrow 0$ for $\rho \rightarrow \infty$.

Next, let us take into account the right-hand side of (50). Since $2\pi\delta(x, y) = \nabla^2 \ln \rho$ and $H_0^{(1)}(\eta\rho) \rightarrow \frac{2i}{\pi} \ln \rho$ for $\rho \rightarrow 0$ we obtain that $\nabla^2 H_0^{(1)} = 4i\delta(x, y) - \eta^2 H_0^{(1)}$. Hence, only zero-order Hankel function contributes to solution of (50),

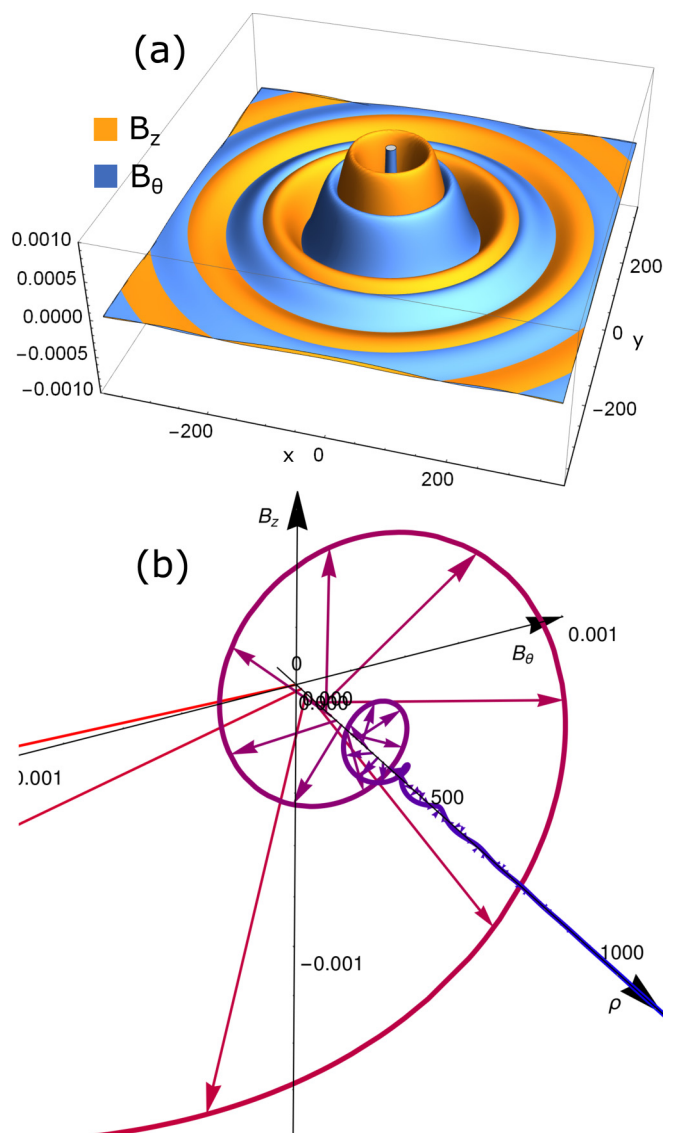


FIG. 1. Magnetic field \vec{B} of a right-handed vortex obtained in the London approximation, which is given by (52) with $\kappa_c = 20$, $\gamma = 20$, $\nu = 1$. (b) Shows \vec{B} on a line going radially along ρ away from the vortex core.

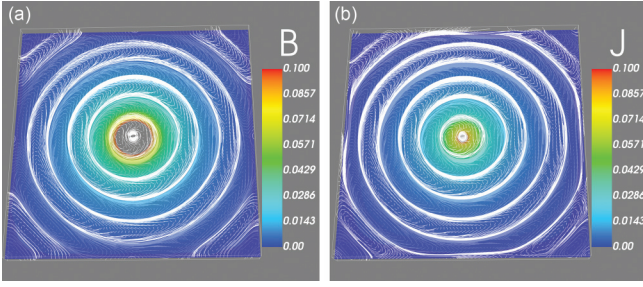


FIG. 2. Vortex obtained numerically in the three-dimensional model (29) with $\kappa_c = 0.3$, $\gamma = 2$, $\nu = 0.1$. (a) White streamlines show the force lines of the magnetic field starting from the middle cross section. The color shows $|\vec{B}|$, which is cut off at $B = 0.1$ for visualization purposes. Note periodical structure in the radial direction, which corresponds to spirals as in the analytic solution, Fig. 1. (b) Streamline plot for current $\vec{J} \equiv \nabla \times \vec{B}$. Observe that the current configuration is very similar to that of the magnetic field. While there is, as usual, current going around the vortex core, there is a part of current going along the vortex core, alternating the direction.

which is given by

$$f = \frac{i\pi}{2} \eta n H_0^{(1)}(\eta\rho). \quad (51)$$

Hence, using (51) and the first line in (45), we obtain the magnetic field of a vortex (see Fig. 1):

$$\vec{B} = \text{Re} \left[\frac{i\pi}{2} n \eta (\eta \vec{e}_z - \vec{e}_z \times \nabla) H_0^{(1)}(\eta\rho) \right]. \quad (52)$$

For $\nu, \gamma \rightarrow 0$ this expression, as expected, gives the usual result $\vec{B} = -\vec{e}_z \frac{n\kappa_0(x/\lambda)}{\lambda^2}$. In polar coordinates, Eq. (52) can be written as

$$\vec{B} = \text{Re} \left[\frac{i\pi}{2} n \eta^2 (0, H_1^{(1)}(\eta\rho), H_0^{(1)}(\eta\rho)) \right]. \quad (53)$$

Then, for $\rho \rightarrow \infty$ since $H_1^{(1)} \rightarrow -iH_0^{(1)} \propto \frac{e^{i\eta\rho}}{\sqrt{\rho}}$ the magnetic field forms the right-handed spirals as in the case of the Meissner state [see below (57)], but instead in a radial

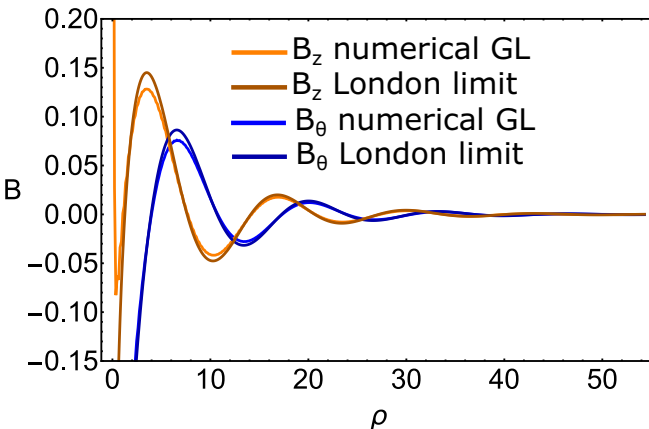


FIG. 3. Comparison of magnetic field of a vortex obtained as full numerical solution of (29) and the London limit analytical solution (52) for $\kappa_c = 0.3$, $\gamma = 2$, $\nu = 0.1$.

direction:

$$\vec{B} = B_z + iB_\theta \propto \frac{e^{i\eta\rho}}{\sqrt{\rho}}. \quad (54)$$

Note, that this is a general observation that decaying magnetic field forms a spiral with handedness determined by the sign of γ .

B. Vortex solution in the Ginzburg-Landau model

To obtain the vortex solution in the full nonlinear Ginzburg-Landau model, we developed a numerical approach that minimizes the free energy (29). For that, we wrote code that uses a nonlinear conjugate gradient algorithm parallelized on CUDA enabled graphics processing unit (for detail of numerical approach, see [27]). The algorithm works as follows: first, the fields ψ and \vec{A} are discretized using a finite-difference scheme on a Cartesian grid. Then, energy is minimized by sequentially updating ψ and \vec{A} in steps. In each step, we calculate gradients of the free energy with respect to the given field. Then, we adjust the resulting vector with a nonlinear conjugate gradient algorithm, which gives the direction of the step in the field. Next, we expand energy in the Taylor series in terms of step amplitude for the obtained step direction. This amplitude is then calculated as a minimizer of the obtained polynomial and the step is made. The discretized grid had $512 \times 512 \times 32$ points. To verify results we used grids of different sizes like 128^3 . The obtained numerical solutions of the full GL model (29) are shown on Fig. 2.

In Fig. 3 we plot a comparison of the analytical solution obtained in the London model and the numerical solution in full nonlinear GL theory.

VI. CROSSOVER TO TYPE-1 SUPERCONDUCTIVITY AT ELEVATED TEMPERATURES

In this section, we show how noncentrosymmetric superconductors can cross over from vortex states at low temperature to type-1 superconductivity at $T \rightarrow T_c$. To that end, let us consider the energy of a single vortex with a core parallel to the z direction. Recall that first critical magnetic field H_{c1} is defined such that vortex energy becomes negative for $H_z \equiv H > H_{c1}$. Namely, vortex energy (per unit length in the z direction) is given by $F_v = 2\pi(H_{c1} - H)$, where H is external magnetic field parallel to the z direction. Next, thermodynamic critical magnetic field H_c is defined as H when energy of the uniform superconducting state $\psi = 1$ and $\vec{A} = 0$ is zero. In our rescaled units, $H_c = 1$. In the usual type-II superconductors, vortices form when $H_{c1} < H_c$. However, as we will see below, the interaction of vortices in this system is nonmonotonic and hence a lattice of vortices will become energetically beneficial for $H'_{c1} < H_{c1}$. Hence, in order to show that superconductor has vortex states it is sufficient to find $H_{c1} < H_c$.

To observe a crossover, consider a noncentrosymmetric superconductor that has $\kappa_c < 1$. Then, at $T \rightarrow T_c$, as we showed above, $\gamma, \nu \rightarrow 0$ and hence it becomes a usual type-1 superconductor described by the GL parameter κ_c . In this case, $H_c < H_{c1}$ and hence vortices are not present. However, when the temperature is decreased, γ and ν increase. By solving

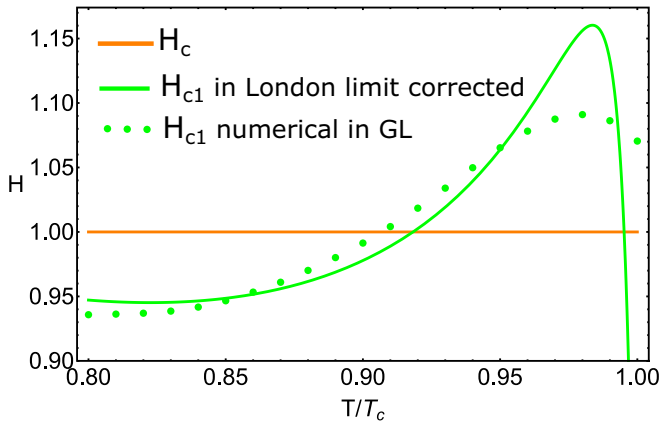


FIG. 4. Crossover between vortex state and type-1 superconductivity in noncentrosymmetric superconductor as a function of temperature. Note that for low temperature, the first critical magnetic field H_{c1} (green dots) is lower than the thermodynamic H_c (orange line) and hence superconductor forms vortices in an external field. For higher temperature $H_{c1} > H_c$, a single vortex cannot be induced by an external magnetic field. For $T \rightarrow T_c$ system becomes usual type-1 superconductor. The calculation in the London limit (55) with a correction for vortex core energy gives quite good approximation $H_{c1} \simeq H_{c1}^L + \frac{0.385}{\kappa_c}$ (green line). Parameters are chosen so that for $T/T_c = 0.9$ they are $\kappa_c = 0.8$, $\gamma = 2.5$, and $\nu = 0.1$. Note that λ/ξ grows as the temperature is decreased. Namely, $\lambda/\xi \simeq 0.89$ for $T/T_c = 1$, whereas at $H_{c1} = H_c$ and $T/T_c \simeq 0.9$ we get $\lambda/\xi \simeq 13$.

the full GL model (29), we find that this leads to a change in the value of H_{c1} . Eventually, it becomes smaller than H_c at sufficiently low temperature (see Fig. 4). This means that vortices will necessarily start to appear.

Next, we study analytically how vortex states become energetically preferable. First, consider the London limit, disregarding the vortex core energy. Using the previously obtained vortex solution (51) and energy given by (49), we obtain energy of a vortex \mathcal{F}_v with winding n . We can express it in terms of the London limit first critical magnetic field H_{c1}^L :

$$\mathcal{F}_v = 2\pi n(nH_{c1}^L + H),$$

$$H_{c1}^L = \frac{\chi}{\kappa_c} \left[\eta_1 \arctan\left(\frac{\eta_1}{\eta_2}\right) + \eta_2 \ln \frac{2e^{-\gamma_{\text{Euler}}}}{|\eta_1 \xi|} \right], \quad (55)$$

where $\gamma_{\text{Euler}} \simeq 0.577 \dots$ is Euler gamma. For a single vortex we have $n = -1$. Let us estimate the core energy of a vortex. Since the vortex core is of size ξ , then it is $\simeq \pi \xi^2 \psi^2 \simeq \frac{\text{const}}{\kappa_c}$ since $\xi = \frac{1}{\sqrt{2\kappa_c}}$ and $\psi \simeq 1$. Hence, the actual first critical magnetic field can be estimated by $H_{c1} \simeq H_{c1}^L + \frac{\text{const}}{\kappa_c}$. When $\kappa_c \gg 1$, γ , ν this core energy is indeed relatively small and can be disregarded.

However, for studying a crossover to type-1 superconductivity (Fig. 4), this is not true since $\kappa_c < 1$. There, instead, the vortex core energy gives a significant contribution to H_{c1} . Numerically, we estimated $H_{c1} \simeq H_{c1}^L + \frac{0.385}{\kappa_c}$ (see Fig. 4). Moreover, from (55) it follows that for the increased value of γ the vortex energy is dominated by core contribution. For the crossover to type-1 superconductivity we need $0.385 \lesssim \kappa_c < 1$ and large enough value of γ .

Finally, consider how parameters γ , ν influence length scales over which order parameter and magnetic field change. Namely, we are interested in the ratio of these scales since for a usual superconductor it determines whether it is of type 1 or type 2. As we showed before [Eq. (33)], coherence length has the usual form in a noncentrosymmetric superconductor. To obtain penetration depth, one needs to solve for Meissner state in the London limit. The Meissner state in the noncentrosymmetric superconductors was discussed before in [11,17,18] for similar models. Here, we rederive it for our model (29) using the method that we outlined in the previous section [Eq. (45)].

Consider superconductor with no vortices occupying half-space $x > 0$ and external magnetic field \vec{H} , parallel to the boundary. As usual, we assume that fields depend only on x . Then, the second equation in (45) is easily solved resulting in $f(x) = ce^{inx}$ since we demand $f(x \rightarrow \infty) \rightarrow 0$, where c is a complex multiplicative constant. To determine c we use boundary condition (34), which in terms of \vec{W} becomes

$$\vec{n} \cdot \text{Im}\vec{W} = 0, \quad \vec{n} \times \text{Re} \left[\frac{i\vec{W}}{\eta} - \frac{\kappa_c}{2\chi} \vec{H} \right] = 0 \quad (56)$$

it gives $c = -\frac{i\kappa_c}{2\chi} \vec{H}$, where $\vec{H} = H_z + iH_y$. From (45) we obtain a magnetic field, which can be represented by a linear combination of components of \vec{B} parallel to the boundary $\vec{B} = B_z + iB_y$:

$$\vec{B} = -\frac{i\eta\kappa_c}{2\chi} \vec{H} e^{inx} \propto e^{-\eta_2 x + i\eta_1 x}. \quad (57)$$

While the magnetic field has a spiral decay, its modulus has an exponential decay (see Fig. 5). That allows to define the penetration depth for magnetic field as the inverse of imaginary part of η :

$$\lambda = \frac{1}{\eta_2}. \quad (58)$$

Importantly, inside a superconductor, the direction of the magnetic field rotates with the period $\frac{2\pi}{\eta_1}$, forming a right-handed spiral (helical) structure. This spiral is shown on Fig. 5. Note that handedness of the state is set by the sign of η_1 . Also observe that the operator $\mathcal{L}\mathcal{L}^*$ that determines the configuration of \vec{B} is invariant under inversion (parity) transformation $\mathbb{P} : \vec{r} \rightarrow -\vec{r}$ and the model is centrosymmetric only if $\eta_1 = 0$. It is also apparent from the fact that $\eta_1 \propto \gamma$, where γ is, as was shown above, the parameter that determines the degree of noncentrosymmetry of the material.

The ratio of the magnetic field penetration length and coherence length for the noncentrosymmetric superconductor then reads as

$$\frac{\lambda}{\xi} = \kappa_c \frac{1 + \frac{2}{\kappa_c}(\gamma^2 + \nu^2)}{\sqrt{1 + \frac{2}{\kappa_c}\nu^2}}. \quad (59)$$

Note that γ , $\nu \propto \sqrt{\ln \frac{T_c}{T}}$ strongly depend on T and go to zero for $T \rightarrow T_c$ [see (30)]. Since $\gamma/\nu \simeq \text{const}$ the ratio λ/ξ increases when temperature is decreased (see Fig. 6). Hence, it is typical that in noncentrosymmetric superconductors $H_c = H_{c1}$ for $\lambda/\xi \neq 1$. Namely, for the parameters in Fig. 4 we

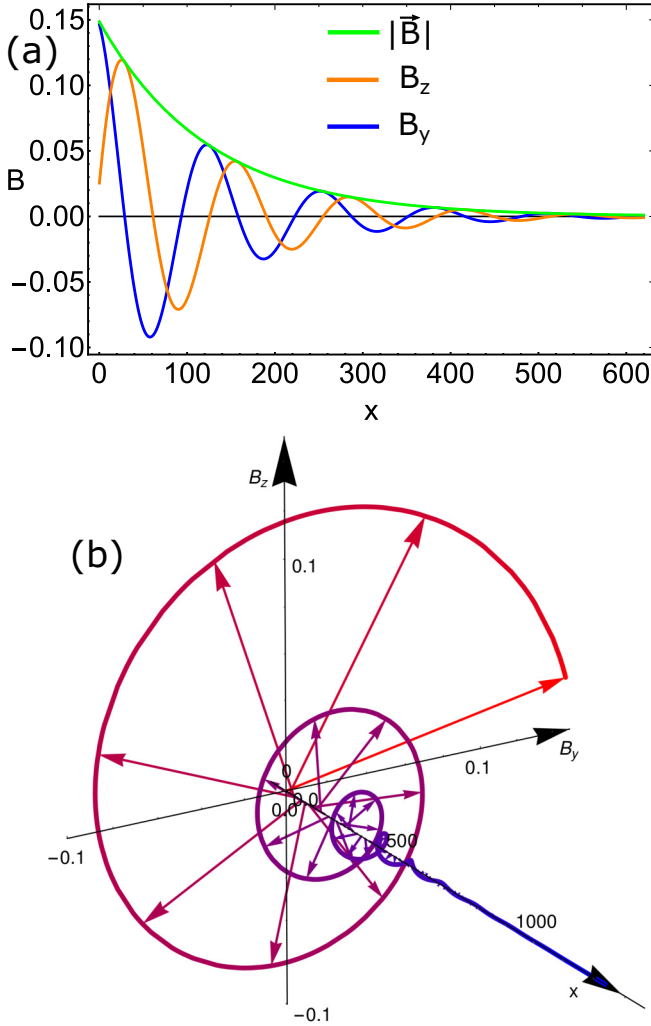


FIG. 5. Magnetic field \vec{B} decay in a superconductor in the right-handed Meissner state. The result is obtained in the London approximation, which is given by (57) with $\kappa_c = 20$, $\gamma = 20$, $\nu = 1$. Superconductor is positioned at $x > 0$. The handedness of the state is determined by the sign of γ .

obtained that $H_c = H_{c1}$ for $\lambda/\xi \approx 13$, which is in strong contrast to centrosymmetric superconductors where $H_c = H_{c1}$ for $\lambda/\xi = 1$ (or $1/\sqrt{2}$ in different units). We show below that interaction between vortices is nonmonotonic and the critical field for vortex clusters is smaller than H_{c1} for a single vortex, and thus there is no Bogomolny point in the noncentrosymmetric superconductors considered in this paper.

We obtained crossover Fig. 4 and Eq. (59) by considering a noncentrosymmetric superconductor with O or T symmetry. Noncentrosymmetric systems with different symmetry have terms of different structure but with the same scaling, corresponding to spin-orbit and Zeeman coupling terms. It means that for any symmetry it is expected to have a strong dependence of these noncentrosymmetric terms on temperature. Consequently, if $\kappa_c < 1$ and γ , ν terms are large enough, one can expect the crossover between different types in noncentrosymmetric superconductors. This type of behavior was reported for noncentrosymmetric superconductor AuBe [13].

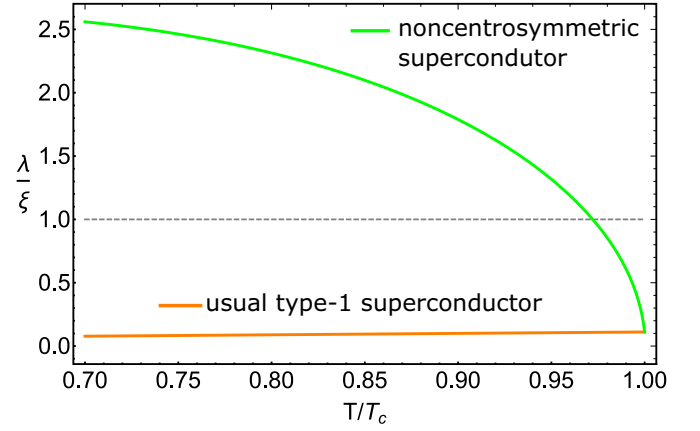


FIG. 6. Ratio of penetration depth and coherence length in noncentrosymmetric superconductor (green) given by (59). In this case the system exhibits type-1 superconductivity, but λ/ξ still changes significantly and it is equal to κ_c for $T/T_c = 1$. For comparison, $\lambda/\xi \equiv \kappa_c$ of the usual superconductor (orange) weakly depends on temperature. Parameters are chosen so that for $T/T_c = 0.9$ they are $\kappa_c = 0.1$, $\gamma = 2$, and $\nu = 2$.

VII. INTERVORTEX INTERACTION AND VORTEX BOUND STATES

Here, we compute the interaction energy of vortices by using (49). Consider a set of vortices with windings n_i placed at \vec{r}_i with cores parallel to \vec{e}_z . Then, according to (45) and single vortex solution (51), f satisfies

$$\begin{aligned} \nabla^2 f + \eta^2 f &= -2\pi\eta \sum_i n_i \delta(x - x_i, y - y_i) \equiv \eta \delta, \\ f &= \sum_i \frac{i\pi}{2} n_i \eta H_0^{(1)}(\eta|\vec{r} - \vec{r}_i|). \end{aligned} \quad (60)$$

Then by using Eq. (60) and its complex conjugate we obtain the energy per unit length in the z direction:

$$\mathcal{F} = \int dx dy \left[-\frac{\chi}{\kappa_c} \text{Im}(f) - H_z \right] \delta, \quad (61)$$

where we also used that the flux of the vortices is fixed by δ . The integral in (61) is easily performed for any vortex combination since δ contains the Dirac deltas in it. Now let us consider only two vortices $i = 1, 2$. By subtracting from (61) energies of single vortices, Eq. (55), we obtain the interaction energy U as a function of distance R between them:

$$U(R) = 2\pi^2 n_1 n_2 \frac{\chi}{\kappa_c} \text{Re}[\eta H_0^{(1)}(\eta R)]. \quad (62)$$

Importantly, the intervortex interaction energy U (see Fig. 7) changes sign. Analytically, asymptotics for big R is given by

$$U(R) \propto n_1 n_2 \frac{e^{-\eta_2 R}}{\sqrt{R}} \cos(\eta_1 R + \phi_0), \quad (63)$$

where $\phi_0 = \frac{\arg[\eta]}{2} - \frac{\pi}{4}$. Hence, the system forms vortex-vortex and vortex-antivortex pairs. Those will form stable states at distances R corresponding to local minima in U . Approximately (for big R), these minima appear with period $\frac{2\pi}{\eta_1}$. Note

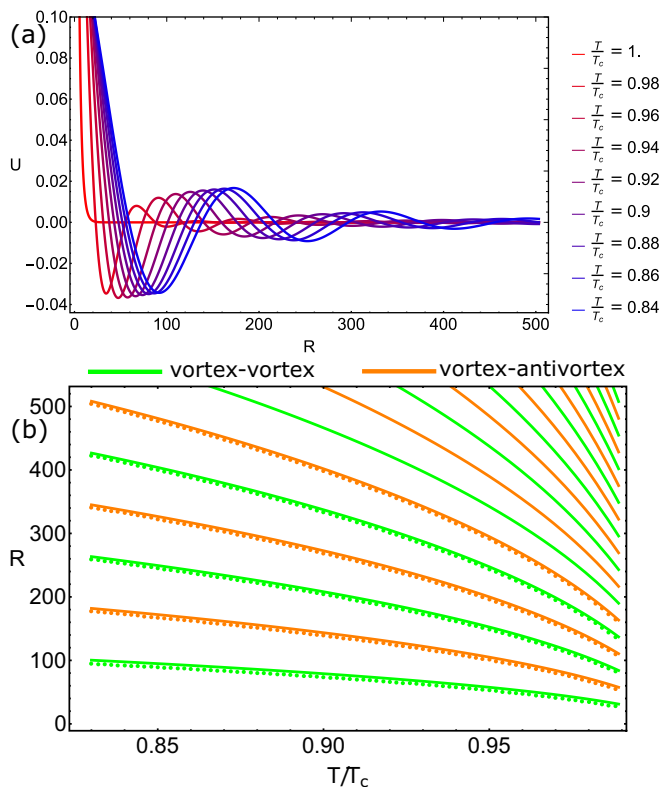


FIG. 7. (a) Vortex-vortex interaction energy U [Eq. (62)] as function of distance between vortices R for several values of temperature T . Parameters chosen so that at $T/T_c = 0.9$ other parameters are $\kappa_c = 20$, $\gamma = 20$, $\nu = 1$. The plot is cut off for small distances and presented for $R > \xi$. Interaction clearly has minima which lead to bound states of vortices. (b) Distance between vortex and vortex (green) and vortex and antivortex (orange) in corresponding bound pairs as a function of temperature. Dots: numerical solutions for extrema of (62). Lines: simplest estimate by (64). For reference, at $T/T_c = 0.9$ first critical magnetic field $H_{c1} \simeq 0.02$.

that for $T \rightarrow T_c$ period $\frac{2\pi}{\eta_1} \rightarrow 0$. The simplest estimate as minima and maxima of \cos in (63) gives

$$R_{VV} = \frac{\pi + 2\pi k - \phi_0}{\eta_1}, \quad R_{VAV} = \frac{2\pi k - \phi_0}{\eta_1}, \quad (64)$$

where R_{VV} is the distance between vortices, R_{VAV} is the distance between vortex and antivortex, and k is an integer.

This behavior is due to the fact that in noncentrosymmetric superconductor vortices are represented by ‘‘circularly polarized’’ cylindrical magnetic field (52) with period approximately equal to $\frac{2\pi}{\eta_1}$ (see Figs. 2 and 8). Two or more of them brought together will form an interference pattern of two-point sources which, when moving them apart, will alternate between in phase and out of phase with the same period.

In the London limit, interaction can be easily generalized to an arbitrary number of vortices. Namely, using (61), pairwise interaction will be given by the same U [Eq. (62)]. Hence, we can suggest that vortices can form lattices with the distance between neighboring vortices given by one of the minima of U [Eq. (62)]. Similarly, lattices of vortices and antivortices can be formed.

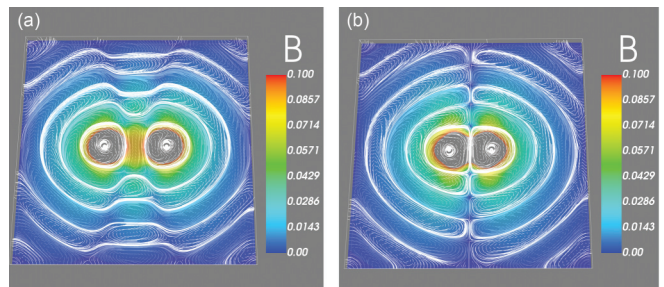


FIG. 8. (a) Vortex-vortex and (b) vortex-antivortex bound states obtained numerically in the three-dimensional model (29) with $\kappa_c = 0.3$, $\gamma = 2$, $\nu = 0.1$. White streamlines show the force lines of the magnetic field starting from the middle cross section. The color shows $|B|$.

We obtained the bound states numerically in the full nonlinear GL model given by (29). Figure 8 shows two examples of such bound states.

VIII. VORTEX-BOUNDARY INTERACTION

In this section, we show that in noncentrosymmetric superconductors the physics of vortex-boundary interaction is unconventional. Consider a half-infinite superconductor positioned at $x > 0$ and right-handed vortex with winding n placed at $x = R$ and $y = 0$. Here we study the problem in the London limit and thus neglect the effects associated with the gap variations near the surface [28], and the nonlinear effects appearing at the scale of the vortex core [29]. External magnetic field is set to be $\vec{H} = (0, 0, H)$. Then, auxiliary field f should satisfy the following equation inside the superconductor [Eq. (45)]:

$$\nabla^2 f + \eta^2 f = -2\pi \eta n \delta(x - R, y) \equiv \eta \delta \quad (65)$$

supplemented by the boundary condition that f is zero at $x \rightarrow \infty$. From (34) or equivalently (56) we obtain the following boundary conditions at $x = 0$:

$$\text{Im}[\eta^* \partial_x f] = 0, \quad \text{Im}[f] = -\frac{\kappa_c}{2\chi} H. \quad (66)$$

Since (65) is linear in f , it is convenient to write the solution as superposition of Meissner state, vortex and image of a vortex as

$$f = f_m + f_v + f_i, \quad f_m = -\frac{i\kappa_c}{2\chi} H e^{inx},$$

$$f_v = \frac{i\pi}{2} n \eta H_0^{(1)}(\eta \sqrt{(x-R)^2 + y^2}), \quad (67)$$

where f_m and f_v were found in the previous sections. Note that since the Meissner state f_m satisfies boundary conditions (66), the vortex and image $f_v + f_i$ should satisfy (66) with zero right-hand side.

Remember that with the London model, for usual superconductor image of the vortex is just its mirror reflection in the boundary, which is modeled by antivortex positioned outside the superconductor (see [30]). This configuration then satisfies both (65) and boundary conditions (66). By contrast in our case for noncentrosymmetric superconductor unfortunately it is not possible to use this approach. Namely, mirror reflection

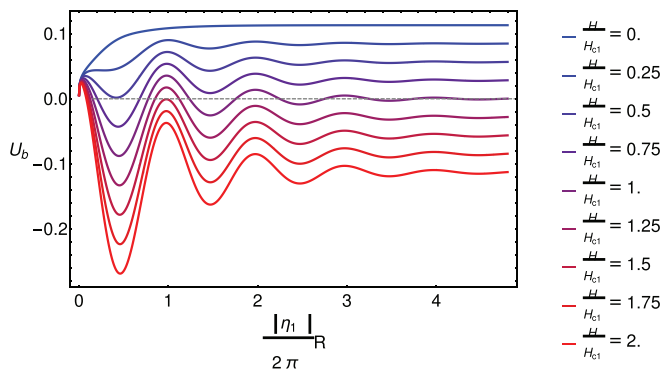


FIG. 9. Energy of a vortex interacting with a boundary U_b [Eq. (70)] for $\kappa_c = 20$, $\gamma = 20$, $\nu = 1$ as function of distance from vortex to boundary R for several values of external magnetic field H . The plot is cut off for small distances and presented for $R > \xi$. Note that compared to the usual superconductor, now the vortex has multiple minima, which are distant from the boundary with period $\frac{2\pi}{|\eta_1|}$ for any nonzero H .

of a right-handed vortex inside the superconductor is a left-handed antivortex outside, which indeed satisfies boundary conditions (66), but the equation for \vec{B} , Eq. (35) [more complicated version of (65)], is not satisfied. This is simply because the antivortex is left handed but the equation is right handed, or vice versa for $\gamma < 0$. Inserted as an image the right-handed antivortex satisfies (65), but not boundary conditions (66).

So to obtain an “image” configuration f_i we have to solve explicitly Eq. (65). We did that by performing Fourier transform in the y direction and solving corresponding equations (65) for $f_v + f_i$ together subjected to boundary condition (66) with zero right-hand side, which gives

$$f_i(x, y) = \frac{1}{2\pi} \int_{-\infty}^{\infty} \tilde{f}_i(x, k) e^{iky} dk,$$

$$\tilde{f}_i(x, k) = -\frac{\pi n \eta}{s} e^{-sx} \left[e^{-s^*R} - 2 \frac{\text{Re}(s\eta^*)}{\text{Im}(s\eta^*)} \text{Im}(e^{-sR}) \right] \quad \text{with}$$

$$s = \sqrt{k^2 - \eta^2}. \quad (68)$$

To obtain energy we integrate by parts (49) and use (65), which gives

$$\mathcal{F} = \int_0^{\infty} dx \int_{-\infty}^{\infty} dy \left[-\frac{\chi}{\kappa_c} \text{Im}(f) - H \right] \delta$$

$$- \int_{-\infty}^{\infty} dy \frac{H}{2} \frac{\partial_x f}{\eta} \Big|_{x=0}, \quad (69)$$

where we obtain, compared to (61), the last term which is boundary integral. Now, inserting solutions (67) and (68) up to constant terms we obtain the energy of a vortex interacting with a boundary (see Fig. 9):

$$U_b(R) = -2\pi n H \text{Re}[e^{i\eta R}] + 2\pi n \frac{\chi}{\kappa_c} \text{Im}[f_i(R, 0)] + \mathcal{F}_v, \quad (70)$$

where \mathcal{F}_v is energy of a single vortex in the bulk of superconductor (55) and other terms represent the interaction energy of vortex and boundary. For a large distance away

from the boundary R , the main contribution to the interaction energy comes from first term in (70) and hence it has similar asymptotics as for vortex-vortex interaction, namely, we obtain $U_b \propto \text{Re}[e^{i\eta R}]$, which has minima with period $\simeq \frac{2\pi}{|\eta_1|}$ (see Fig. 9).

Physically, it means that the vortex-surface interaction in a noncentrosymmetric superconductor is principally different from that in an ordinary one. Namely, in the latter case the interaction with a boundary is barrierlike for nonzero fields and attractive for zero and inverted fields [29–33]. By contrast, we found that in a noncentrosymmetric superconductor, vortices should form a bound state with a boundary. Then, in increasing magnetic field vortices will first tend to stick near the boundary and only when there will be a considerable amount of them occupying these minima vortices will be pushed into the bulk of superconductor in the form of multivortex bound state.

For $\gamma \rightarrow 0$, f_i in the second term in (70) corresponds to an antivortex as in [30]. But, physical interpretation in [30] of the first term in (70) as Meissner-vortex and the second term as vortex-image interactions is not fully justified. First, when integrating by parts energy [Eq. (49)] these terms are obtained from combining energy and flux from the field configuration of vortex and image. Second, half of the first term in (70) comes from boundary integral in (69) due to vortex-image interaction.

IX. CONCLUSIONS

We considered the physics of magnetic field behavior and vortex states in noncentrosymmetric superconductors. We microscopically derived a Ginzburg-Landau model for noncentrosymmetric superconductors which does not suffer from unphysical ground-state instability, which was present in frequently used phenomenological models. The main conclusion of the microscopic part of the paper is that type of magnetic response in a noncentrosymmetric superconductor has significant temperature dependence and one can expect materials that are type 1 close to critical temperature to exhibit vortex states at lower temperatures. We find that the first critical magnetic field for the single-vortex entry H_{c1} becomes equal to the thermodynamical critical magnetic field at very different ratios of magnetic field penetration length to coherence lengths than in ordinary superconductors, and there is no Bogomolny point at $\lambda/\xi = 1$.

The multivortex states in these systems are unconventional. The demonstrated spiral-like decay of the magnetic field away from a vortex leads to multiple minima in the intervortex interaction potentials and thus the formation of bound states of vortices and stable vortex-antivortex bound states.

We find that vortices have a similar oscillating sign of interaction with Meissner current close to the boundaries, and form bound states with boundaries. The properties may potentially be utilized for new types of control of vortex matter for fluxonics and vortex-based cryocomputing applications.

Note added. Similar results are obtained by Garaud, Chernodub, and Kharzeev in Ref. [34].

ACKNOWLEDGMENTS

We thank F. N. Rybakov and J. Garaud for the discussions. The work was supported by the Swedish Research

Council Grants No. 642-2013-7837, No. 2016-06122, No. 2018-03659, and Göran Gustafsson Foundation for Research in Natural Sciences and Medicine and Olle Engkvists Stiftelse.

-
- [1] F. London, *Superfluids: Macroscopic Theory of Superconductivity*, Vol. 1 (Dover, New York, 1961).
- [2] M. Tinkham, *Introduction to Superconductivity* (Dover, New York, 2004).
- [3] B. V. Svistunov, E. S. Babaev, and N. V. Prokof'ev, *Superfluid States of Matter* (CRC Press, Boca Raton, FL, 2015).
- [4] L. D. Landau and V. Ginzburg, *Zh. Eksp. Teor. Fiz.* **20**, 1064 (1950).
- [5] E. Babaev and M. Speight, *Phys. Rev. B* **72**, 180502(R) (2005).
- [6] M. Silaev and E. Babaev, *Phys. Rev. B* **84**, 094515 (2011).
- [7] J. Carlström, J. Garaud, and E. Babaev, *Phys. Rev. B* **84**, 134518 (2011).
- [8] J. Carlström, E. Babaev, and M. Speight, *Phys. Rev. B* **83**, 174509 (2011).
- [9] E. Babaev, J. Carlström, M. Silaev, and J. Speight, *Physica C (Amsterdam)* **533**, 20 (2017).
- [10] M. Silaev, T. Winyard, and E. Babaev, *Phys. Rev. B* **97**, 174504 (2018).
- [11] E. Bauer and M. Sigrist, *Noncentrosymmetric Superconductors: Introduction and Overview*, Vol. 847 (Springer, New York, 2012).
- [12] S. Yip, *Annu. Rev. Condens. Matter Phys.* **5**, 15 (2014).
- [13] D. J. Rebar, S. M. Birnbaum, J. Singleton, M. Khan, J. C. Ball, P. W. Adams, J. Y. Chan, D. P. Young, D. A. Browne, and J. F. DiTusa, *Phys. Rev. B* **99**, 094517 (2019).
- [14] T. Shang, M. Smidman, A. Wang, L.-J. Chang, C. Baines, M. K. Lee, Z. Y. Nie, G. M. Pang, W. Xie, W. B. Jiang, M. Shi, M. Medarde, T. Shiroka, and H. Q. Yuan, *Phys. Rev. Lett.* **124**, 207001 (2020).
- [15] A. D. Hillier, J. Quintanilla, and R. Cywinski, *Phys. Rev. Lett.* **102**, 117007 (2009).
- [16] Arushi, D. Singh, P. K. Biswas, A. D. Hillier, and R. P. Singh, *et al.*, *Phys. Rev. B* **101**, 144508 (2020).
- [17] L. S. Levitov, Yu. V. Nazarov, and G. M. Eliashberg, *Pisma Zh. Eksp. Teor. Fiz.* **41**, 365 (1985) [*JETP Lett.* **41**, 445 (1985)].
- [18] C.-K. Lu and S. Yip, *Phys. Rev. B* **77**, 054515 (2008).
- [19] V. P. Mineev and K. V. Samokhin, *Phys. Rev. B* **78**, 144503 (2008).
- [20] K. V. Samokhin, *Phys. Rev. B* **70**, 104521 (2004).
- [21] K. V. Samokhin and V. P. Mineev, *Phys. Rev. B* **77**, 104520 (2008).
- [22] C.-K. Lu and S. Yip, *Phys. Rev. B* **78**, 132502 (2008).
- [23] M. K. Kashyap and D. F. Agterberg, *Phys. Rev. B* **88**, 104515 (2013).
- [24] We thank Fillipp N. Rybakov for pointing that out.
- [25] S. Chandrasekhar and P. C. Kendall, *Astrophys. J.* **126**, 457 (1957).
- [26] K. V. Samokhin, *Phys. Rev. B* **89**, 094503 (2014).
- [27] A. Samoilenka, F. N. Rybakov, and E. Babaev, *Phys. Rev. A* **101**, 013614 (2020).
- [28] A. Samoilenka and E. Babaev, *Phys. Rev. B* **101**, 134512 (2020).
- [29] A. Benfenati, A. Maiani, F. N. Rybakov, and E. Babaev, *Phys. Rev. B* **101**, 220505 (2020).
- [30] C. Bean and J. Livingston, *Phys. Rev. Lett.* **12**, 14 (1964).
- [31] L. Kramer, *Phys. Rev.* **170**, 475 (1968).
- [32] L. Kramer, *Z. Phys. A: Hadrons Nucl.* **259**, 333 (1973).
- [33] P. de Gennes, *Rev. Mod. Phys.* **36**, 225 (1964).
- [34] J. Garaud, M. N. Chernodub, and D. E. Kharzeev, *Phys. Rev. B* **102**, 184516 (2020).